Proc. Natl. Acad. Sci. USA
Vol. 96, pp. 11589–11594, September 1999
Neurobiology

Slow transport of unpolymerized tubulin and polymerized neurofilament in the squid giant axon

(slow axonal transport/diffusion/axoplasmic transport/cytoskeleton)

JAMES A. GALBRAITH*†‡, THOMAS S. REESE*†, MICHELLE L. SCHLIEF*†, AND PAUL E. GALLANT*†‡

*Laboratory of Neurobiology, National Institute of Neurological Disorders and Stroke, National Institutes of Health, Bethesda, MD 20892-4062; and †Marine Biological Laboratory, Woods Hole, MA 02543

Contributed by Thomas S. Reese, July 23, 1999

ABSTRACT **A major issue in the slow transport of cytoskeletal proteins is the form in which they are transported. We have investigated the possibility that unpolymerized as well as polymerized cytoskeletal proteins can be actively transported in axons. We report the active transport of highly diffusible tubulin oligomers, as well as transport of the less diffusible neurofilament polymers. After injection into the squid giant axon, tubulin was transported in an anterograde direction at an average rate of 2.3 mm/day, whereas neurofilament was moved at 1.1 mm/day. Addition of the metabolic poisons cyanide or dinitrophenol reduced the active transport of both proteins to less than 10% of control values, whereas disruption of microtubules by treatment of the axon with cold in the presence of nocodazole reduced transport of both proteins to ≈20% of control levels. Passive diffusion of these proteins occurred in parallel with transport. The diffusion coefficient of the moving tubulin in axoplasm was 8.6 $\mu m^2/s$ compared with only 0.43 $\mu m^2/s$ for neurofilament. These results suggest that the tubulin was transported in the unpolymerized state and that the neurofilament was transported in the polymerized state by an energy-dependent nocodazole/cold-sensitive transport mechanism.**

Most axonal proteins must be synthesized in neuronal cell bodies that lie many centimeters away. Because passive diffusion is an ineffective means of delivering proteins at distances of a millimeter or more (1), various active transport mechanisms have evolved to convey proteins along the axon. Most cytoplasmic proteins are transported at rates between 1 and 4 mm/day by an unknown slow transport mechanism (2, 3). Slow transport has been studied most extensively with *in vivo* models where radioactively labeled amino acids are injected near neuronal cell bodies for incorporation into neuronal proteins. After days or weeks the distribution of the radiolabeled proteins is mapped and rates are calculated (2, 4–6). While this approach has been adequate to characterize the general parameters of slow transport, it has not served to determine the precise form of the transported material, the motor(s) that power it, or the tracks that guide it.

To better understand slow transport, a number of attempts have been made to visualize slow transport of fluorescently labeled cytoskeletal proteins *in vitro*, typically in cultured neurons (7–11). Cultured neurons provide a system that allows for good control over the form of the materials injected and a signal that can be directly observed in real time as compared with radioactively labeled *in vivo* systems, where only a single time point is obtained from each experiment. The *in vitro* experiments have clearly detected the diffusion of tubulin, actin (12), and neurofilament (13) subunits but have not as clearly demonstrated the active transport of these cytoskeletal proteins.

We have used the squid giant axon as an alternative to cultured neurons to investigate the active movement of cytoskeletal proteins. Previously we demonstrated that the squid giant axon could transport microtubules that were artificially stabilized with paclitaxel (14). In the present experiments we used the squid giant axon to demonstrate that unpolymerized tubulin and polymerized neurofilaments are also moved anterogradely at slow transport rates.

MATERIALS AND METHODS

Squid (*Loligo pealeii*) were obtained daily from the Marine Resources Center of the Marine Biological Laboratory, Woods Hole, MA. The hindmost stellar nerve was dissected under running seawater, and a 4- to 6-mm segment was cleaned of small nerve fibers and loose connective tissue. Axons that exhibited any damage after this procedure were discarded (15).

Axons were injected with rhodamine-labeled neurofilaments or tubulin (Cytoskeleton, Denver, CO) as previously described by using front-loaded pressure pipettes whose tips were broken to yield diameters of approximately 1–3 μm (14). The only differences were use of dimethylpolysiloxane oil (Sigma) as the damping fluid in the pipette and mounting of the axon on the stage of a Zeiss Stemi DRC dissecting microscope with dark-field illumination for injection. Axons that developed a white spot indicative of damage at the injection site were discarded.

After injection, the axon was transferred to an observation chamber that was perfused with fresh solution at 15-min intervals. A laser scanning confocal imaging system (Bio-Rad MRC 600) attached to an upright Zeiss Axioplan was used to image the fluorescent material immediately after injection. The axon was observed by simultaneous transmitted light and fluorescence by using either a Plan-neofluor 10× 0.3-numerical aperture (n.a.) or an Achroplan 4× 0.1-n.a. lens. The equator of the oil drop was used as the focal plane and the confocal microscope's pinhole was set to obtain an optical section between ≈20 and 75 μm thick.

Experiments were performed at room temperature in artificial seawater (ASW) consisting of 423 mM NaCl, 9 mM KCl, 9 mM $CaCl_2$, 23 mM $MgCl_2$, 25 mM $MgSO_4$, 11.1 mM dextrose, and 10 mM Hepes, pH 7.4. To determine whether cytoskeletal movement was energy dependent, either 2 mM cyanide or 1 mM 2,4-dinitrophenol (DNP) was added to the bath (15) in some experiments. Results were the same with either poison. In experiments that tested the dependency of transport on microtubules, the microtubules in the axon were depolymerized as follows. Axons were incubated in ASW with 150 nM

The publication costs of this article were defrayed in part by page charge payment. This article must therefore be hereby marked "*advertisement*" in accordance with 18 U.S.C. §1734 solely to indicate this fact.

PNAS is available online at www.pnas.org.

‡To whom reprint requests may be addressed at: Laboratory of Neurobiology, Bldg. 36, 2A21, National Institutes of Health, Bethesda, MD 20892-4062. E-mail: jgalbrai@codon.nih.gov or gallant@codon.nih.gov.

methyl-[5-(2-thienylcarbonyl)-1*H*-benzimidazol-2-yl] carbamate (nocodazole) for 30 min and then exposed to cold (−2°C) for 5 min in ASW. Nocodazole (150 nM) was present in the ASW for the duration of the experiments to prevent repolymerization of the cold-depolymerized microtubules. This combination of cold and nocodazole was selected experimentally because it stopped microtubule-dependent fast axonal transport (16, 17) but did not degrade the axoplasm or swell the mitochondria (18) when viewed with high numerical aperture differential interference contrast microscopy.

Rhodamine-labeled neurofilaments and tubulin were prepared for injection by diluting a 2-μl aliquot of protein with 2–3 μl of distilled water. The neurofilament aliquot was not centrifuged to remove particles that might clog the pipette because some of the fluorescent neurofilament protein is pelleted by centrifugation. The tubulin was thawed on ice before the distilled water was added, and was spun for 10 min at 14,000 × *g*. The fluorescent tubulin remained in the supernatant after centrifugation. Both the neurofilament and tubulin were kept on ice for a minimum of 30 min before loading into the pipette. The volume of neurofilament or tubulin injected averaged 400 picoliters (pl), while the volume of the oil drop was roughly 25 pl. To ensure that only unpolymerized tubulin was being studied, the tubulin preparation in some instances was spun at 100,000 × *g* to remove any minor polymeric fraction. In these experiments axons were pretreated and maintained in 150 nM nocodazole without cold to prevent the injected unpolymerized tubulin from polymerizing in the axon.

To determine the polymerization state of the neurofilament and tubulin proteins before they were injected into the axon these proteins were spun at 100,000 × *g* on a Airfuge ultracentrifuge (Beckman). Negative stain, SDS/PAGE, and fluorimetry were used to examine the resulting pellets and supernatants. Negatively stained samples were prepared by absorbing the sample onto carbon-coated grids, stained with uranyl acetate, and then examined with a JEOL 100-CX electron microscope. The proteins in the pellet and supernatant were also examined by SDS/PAGE followed by Coomassie blue staining. The total fluorescence of the 100,000 × *g* pellet and supernatant fractions were measured with a model 650–10S Perkin–Elmer fluorimeter.

Transport rates and diffusion coefficients were determined by analyzing a nonsaturated intensity profile from a line drawn through the fluorescent material along the axis of the axon by using NIH IMAGE 1.62 (Wayne Rasband, National Institutes of Health; available at http://rsb.info.nih.gov/nih-image/) on an Apple Macintosh G3 computer. For rate determinations, the center of the oil drop was used as a fixed reference marker because it has been shown to remain stationary after injection (14). The peak of the moving wave was taken as the maximum value of the fluorescence.

Diffusion was analyzed assuming one-dimensional diffusion along a cylinder from a finite source: $C = M/2(\pi Dt)^{1/2} \exp(-x^2/4Dt)$, where M is the total material injected, D is the diffusion coefficient, t is time, and x is distance from the peak of the signal (19). Concentration, C, was considered to be proportional to fluorescent intensity, so that at each time point the intensity curve was fitted by least squares to determine the diffusion coefficient. Four to six time points were used for each experiment to obtain the diffusion coefficient for a particular axon. Diffusion coefficients of the fluorescently labeled proteins were also determined in aqueous solution by observing the spread of these molecules after they were injected into a capillary tube filled with buffer mimicking the intracellular ionic environment in squid (15, 18).

RESULTS

After injection of the rhodamine-labeled neurofilament protein a small intense area of fluorescent material surrounded the nonfluorescent oil drop (Fig. 1*B*). Previous experiments (14) showed that a coinjected oil drop did not move over time, providing a stationary marker of the injection site (Figs. 1 and 2, *A* and *E*). Within 30 min, a significant anterograde plume, or elongation, of the neurofilament fluorescent signal appeared on the side away from the cell body. By 3 hr this fluorescent plume extended anterogradely (left to right in Fig. 1) well beyond the original injection site (Fig. 1 *B* vs. *C*). The peak of this moving fluorescent wave advanced anterogradely at a rate of 47.5 ± 6.4 μm/hr (mean ± SD) (Fig. 1*D*; Table 1, Neurofilament entry).

Table 1. Transport rates of tubulin and neurofilament proteins

Protein	Peak rate, μm/hr
Tubulin	93.9 ± 15.8 (7)
Tubulin/Noc	95.0 ± 19.0 (7)
Tubulin/MP	3.33 ± 9.87* (6)
Tubulin/Noc + cold	12.9 ± 10.9* (6)
Neurofilament	47.5 ± 6.41 (8)
Neurofilament/MP	2.86 ± 7.19* (7)
Neurofilament/Noc + cold	10.5 ± 7.95* (6)

Transport rates were determined in normal axons, metabolically poisoned axons (MP), and axons that had their microtubules disrupted (Noc + cold). Transport rates in control axons were greater (*, $P < 0.001$) than either metabolically poisoned or nocodazole + cold axons. There was no difference between the control tubulin axons and those treated with nocodazole (Noc). Values are mean ± SD with the number of axons in parenthesis.

The injected-rhodamine labeled tubulin spread much more rapidly and extensively in all directions than did the neurofilament protein. In addition to this homogeneous expansion, the fluorescent tubulin also moved as a coherent wave in the anterograde direction (Fig. 2 *B* and *C*) at a rate significantly higher than that of the neurofilament. The anterograde velocity of the tubulin peak was 93.9 ± 16 μm/hr (Fig. 2*D*; Table 1 Tubulin entry). In axons where the injected tubulin was prevented from polymerizing by preexposure to 150 nM nocodazole but not to cold, anterograde movement of the peak occurred at a rate of 95.0 ± 19 μm/hr (Table 1 Tubulin/Noc entry), not statistically different from the rate of transport in axons not treated with nocodazole.

To determine whether the slow movement of neurofilament or tubulin proteins was energy dependent, axons were treated with cyanide or dinitrophenol after they were injected. These metabolic poisons (MP) inhibited most of the anterograde transport of both the neurofilament and tubulin proteins (Figs. 1 and 2 *G* and *H*). After injection, both the fluorescent tubulin and neurofilament spread out symmetrically from around the injection site but there was no significant translation of the injected material in either the anterograde or retrograde direction relative to the oil drop (Figs. 1 and 2 *H* and Table 1 MP entries). Inhibition of movement was reversible; axons that were returned to a bath containing normal ASW resumed their slow anterograde transport within 30 min (data not shown).

Because fast transport requires the presence of microtubules, and can be inhibited by depolymerizing microtubule tracts, we tested the possibility that slow transport might also be sensitive to microtubule depolymerization (20). Microtubules can be shortened or depolymerized with cold (21, 22) and prevented from repolymerizing with nocodazole (20). We used the combination of cold and nocodazole to depolymerize the microtubules and prevent them from repolymerizing during the experiment. The anterograde movement of tubulin and neurofilament protein was significantly, though not completely, inhibited by the 150 nM nocodazole plus cold treatment (Table 1, Tubulin/Noc + cold entry). Neither brief cooling followed by rewarming nor the addition of nocodazole alone stopped transport.

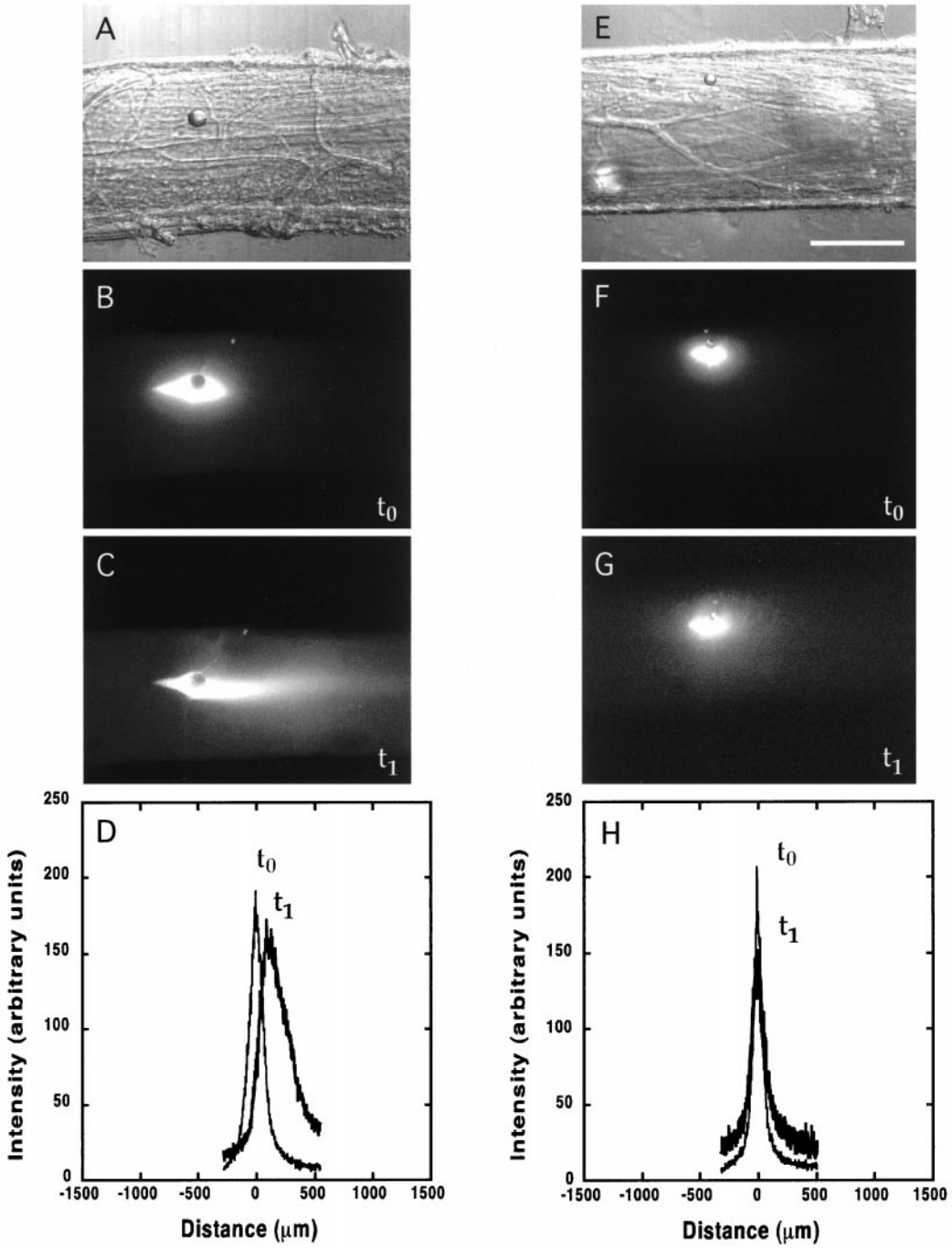

FIG. 1. Active transport and diffusion of fluorescently labeled neurofilament proteins in normal (*A–D*) and metabolically poisoned (*E–H*) squid giant axons. The metabolically poisoned axons show a small amount of spreading but no anterograde movement of the neurofilament. (*A* and *E*) Bright-field image showing the oil drop injected into the axon. (*B* and *F*) Fluorescent image of the neurofilament protein distribution soon after injection (t_0). The oil drop is visible as a dark circle surrounded by bright neurofilament fluorescence. (*C* and *G*) Fluorescence distribution 3 hr later (t_1), showing the anterograde (to the right) movement of the neurofilament protein in *C*. (*D* and *H*) Intensity trace of the neurofilament fluorescence. The axis is centered on the oil drop. (The scale bar in *E* is 250 μm for all images.)

To determine the state of polymerization of the injected tubulin and neurofilament, the injectates were analyzed by centrifugation and electron microscopy, and the diffusional properties of the proteins were measured. Electron microscopy of negatively stained preparations revealed no formed microtubules in the tubulin preparation, but it did show many short intermediate filament fragments in the neurofilament preparation before injection (not shown). Differential centrifugation of these preparations confirmed the soluble nature of the tubulin preparation, since more than 95% of the fluorescent tubulin remained in the supernatant as determined by measures of total fluorescence and SDS/PAGE of the soluble and resuspended tubulin pellet after 1 hr of centrifugation at 100,000 × *g*. Neurofilament, on the other hand, appeared to be mostly polymerized into some individual 10-nm-wide filaments as well as large complexes of self-associated tangles composed of 10-nm-wide filaments. After centrifugation at 100,000 × *g* about half of the fluorescent signal was found in the pellet, whereas the other half was still in the supernatant. The pellet was composed of large clumps of self-associated filaments, whereas the supernatant contained short ≈10-nm-wide filaments when visualized with electron microscopy. SDS/PAGE

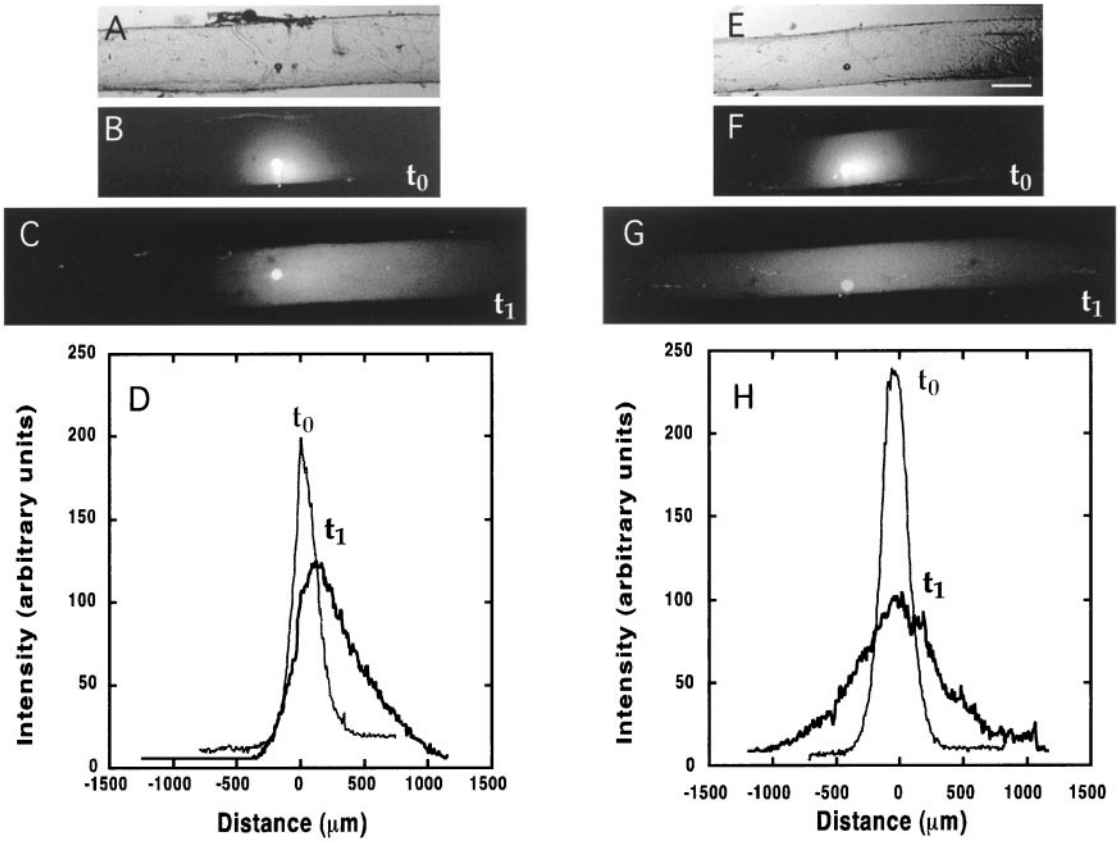

FIG. 2. Active transport and diffusion of fluorescently labeled tubulin proteins. Note that tubulin diffused much more extensively than the neurofilament shown in Fig. 1. The images are arranged as in Fig. 1: *A* and *E*, bright-field; *B* and *F*, fluorescent image soon after injection; *C* and *G*, 3 hr later; and *D* and *H*, trace of fluorescence intensity. (The scale bar in *E* is 250 μm for all images; length scales of the intensity traces are the same as Fig. 1.)

confirmed that the neurofilament protein was divided equally between the pellet and the supernatant. The large clumps may account for the failure of some neurofilament protein to diffuse or move out of the injection site, because at some size material becomes too large to diffuse in cytoplasm (23), and probably even too large to be transported through axoplasm.

Diffusion coefficients were determined for both proteins to calculate their apparent hydrodynamic radius before as well as after injection (Table 2). The hydrodynamic radius, R_h, of tubulin and neurofilaments in buffer was calculated with the values for D_{buffer} and the Stokes–Einstein equation: $D = kT/6\pi\eta R_h$, where D is the diffusion coefficient, k is the Boltzmann constant, η is the solvent viscosity at the experimental temperature (20°C), and T is the temperature in kelvin) (24). We estimated an average hydrodynamic radius of 5.3 ± 1.5 nm for the tubulin and 50.8 ± 20.3 nm for the neurofilament proteins. This calculation suggests that in the intracellular buffer, tubulin was largely unpolymerized, whereas the neurofilament protein was largely polymerized.

Table 2. Diffusion coefficients for tubulin and neurofilament proteins in the squid giant axon and in buffer solution

	D, $\mu m^2/s$	
Exp.	Tubulin	Neurofilament
Axon	8.591 ± 1.706 (7)	0.429 ± 0.345 (8)
Axon/Noc	10.39 ± 1.582 (7)	
Axon/MP	8.852 ± 1.820 (6)	0.253 ± 0.148 (7)
Buffer	43.44 ± 13.92 (6)	4.730 ± 1.720 (8)

The diffusion coefficients did not differ between normal axons and those that were metabolically poisoned (MP) or treated with nocodazole (Noc) ($P > 0.05$). Values are mean ± SD with the number of axons in parenthesis.

Diffusion coefficients were also determined for the tubulin and neurofilament protein after they were injected into metabolically poisoned axons. As illustrated in Fig. 2*G*, tubulin spread out to a much greater extent than the neurofilament, which remained close to the injection site. This behavior is reflected in the diffusion coefficients (Table 2); tubulin's diffusion coefficient is approximately 20 times greater than that of neurofilament. The diffusion coefficients of both proteins were also calculated in actively transporting axons from the broadening of the moving fluorescent protein peaks and were found to be similar to those in the poisoned axons.

The movement of material in a medium is in part determined by the viscosity, which can be approximated as $\eta_{axoplasm} = \eta_{buffer}(D_{buffer}/D_{axoplasm})$. For axoplasm this yields an apparent viscosity of between 5 and 11 centipoise, depending upon the size of the probe. These results are consistent with axoplasm behaving as a non-Newtonian fluid to the diffusing tubulin and neurofilament proteins (25, 26). The viscosity values that we calculate are nominally an order of magnitude more than those for a purely aqueous environment and agree with published neuronal viscosities determined by using known dextrans and electron spin resonance (25, 27).

DISCUSSION

The need for an accessible *in vitro* model of slow axonal transport has long been recognized, but difficult to achieve. Although the slow transport of axonal proteins has been clearly demonstrated *in vivo* (2, 6, 28, 29), it has proven to be difficult to determine the mechanism of slow transport, or even the state in which axonal proteins are transported (30, 31). We propose that many of the defining characteristics of slow transport (2) can be observed *in vitro* in the squid giant axon,

as demonstrated by the anterograde movement of injected fluorescently labeled neurofilament and tubulin proteins at net rates typical of slow transport. The diffusion coefficients of the neurofilament and tubulin proteins indicate that the injected neurofilament is in a polymerized state, whereas the tubulin remains unpolymerized. Although transport of entities falling within the size range of polymers has been reported (14), we are not aware of any observations of transport of highly diffusible protein oligomers.

Requirements for Active Transport of Tubulin and Neurofilament Proteins. The active transport of tubulin and neurofilament was manifested as an anterograde movement of the peak of the fluorescent signal. Tubulin moved at 93.9 ± 15.8 μm/hr ($\approx$2.3 mm/day), whereas the neurofilament peak moved at 47.5 ± 6.4 μm/hr ($\approx$1.1 mm/day), which is similar to the characteristic rates of slow transport measured *in vivo* (2, 29).

The slow transport of both tubulin and neurofilament was over 90% inhibited by metabolic poisons, suggesting that transport is an energy-dependent process. The reversibility of this block indicates that it was due not to secondary damage caused by energy depletion, but rather to the absence of high-energy nucleotides needed to power the slow transport motor(s). Thus, transport of the tubulin and neurofilament entities depends on an active metabolic process.

Tubulin and neurofilament transport was largely inhibited by the combined cold and nocodazole treatment, but not by nocodazole or cold alone. We presume this behavior is because nocodazole and cold together lead to the permanent depolymerization of microtubules, but neither by itself can maintain endogenous microtubules in a depolymerized state. Because axonal microtubules have a slow turnover rate (32), a polymerization-blocking drug such as nocodazole (33) would not be expected to lead to significant depolymerization of microtubules by itself. Likewise, brief cold treatment (21) alone would not be expected to lead to permanent depolymerization of microtubules because the cold-depolymerized microtubules would repolymerize when the axons are rewarmed. However, cold and nocodazole together would depolymerize microtubules and thus inhibit any microtubule-dependent movement. The small amount of transport that persisted even after the combined cold/nocodazole treatment may have been due the existence of cold-insensitive microtubules (21) in axons.

These results suggest that a microtubule-based motor such as kinesin or dynein may be responsible either directly or indirectly for the slow anterograde movement of tubulin and neurofilament. However, the possibility of a myosin-based motor (34) cannot be ruled out because the integrity of the actin tracts necessary for this type of motor function may be sensitive to disassembly of associated microtubules (35). Because the squid axon is easily accessible to pharmacological and biochemical manipulation, experiments designed to test which motor(s) are responsible for slow transport now appear to be feasible.

Polymerization State of Neurofilament and Tubulin Proteins. The present results suggest that tubulin was unpolymerized and neurofilament was polymerized before injection and remained so after injection. When tested in buffered media, the protein's diffusional properties produced an effective hydrodynamic radius for tubulin of $\approx$5 nm and neurofilament of $\approx$51 nm. This behavior leads us to conclude that before injection, tubulin is predominately unpolymerized, whereas the neurofilament is mainly polymerized. This conclusion is also compatible with our ability to visualize by electron microscopy short filaments $\approx$10 nm in diameter in negatively stained samples of neurofilament injectate and with our inability to visualize formed microtubules in the tubulin injectate. The presumption that the tubulin was unpolymerized at the time of injection is also consistent with previous reports that tubulin exists primarily as dimers and small oligomers at room temperature (36).

The diffusion of the tubulin and neurofilament after injection suggested that the tubulin remained unpolymerized and the neurofilament remained polymerized. The diffusion coefficients measured in the axoplasm of actively transporting axons were, as expected, much less than in buffer for tubulin ($\approx$9 $\mu m^2/s$ vs. 43 $\mu m^2/s$) and for neurofilament ($\approx$0.4 $\mu m^2/s$ vs. 5 $\mu m^2/s$). This diminished diffusion could result either from the intrinsically higher viscosity of axoplasm compared with aqueous buffer or from a change in the polymerization state of the proteins. Since the diffusion coefficients of the injected tubulin and neurofilament lead to calculated axoplasmic viscosities that are consistent with measurements of axoplasm in other neurons (25, 27), we conclude that the proteins did not change their polymerization state.

The diffusional measurements alone do not eliminate the possibility that a small fraction of the neurofilament depolymerized or tubulin polymerized and traveled for a short distance before returning to its original form. However, it is likely that neurofilaments are transported in the polymerized state because neurofilaments are very stable and unlikely to depolymerize in axons (37). It is also clear that tubulin can be transported in the unpolymerized state. This was demonstrated by the transport of tubulin that was made polymer-free (by centrifugation at $100{,}000 \times g$ for 1 hr) and kept from polymerizing (by pretreatment with 150 nM nocodazole) once in the axon. The movement of unpolymerized tubulin by simultaneous diffusion and active transport suggests that that the coupling between the motor and tubulin is either loose or intermittent.

Although the movement of small oligomeric or soluble tubulin has previously been hypothesized, the slow transport of unpolymerized tubulin has not previously been observed. Earlier studies in cultured cells detected mostly stationary proteins and highly diffusible fluorescent proteins, but they did not observe transport (12, 38). In the few instances where a transport signal was detected, it did not appear to correspond to the transport of soluble proteins, because there was little or no concomitant spreading or diffusion of the signal (39). The movement of soluble proteins has also not been discernible *in vivo* because these studies depend on multiaxonal nerves whose potentially different rates of axonal transport confound accurate measurements of diffusion (6, 40). An advantage of the squid giant axon model is that diffusion and slow transport can be assessed concomitantly in the same axon.

Relative Contributions of Diffusion and Active Transport. Because nerve cells synthesize material in the cell body there should be a continuous concentration gradient down the axon, making diffusion a de facto transport mechanism, even when active transport is necessary to supply material to points too distant for diffusion to satisfy. In our experiments simultaneous diffusion and active transport were observed moving fluorescent proteins down the axon, whereas previous work has focused on either diffusion or transport, but not both. Indeed, the inherent length limitations of many systems may not allow an adequate separation of the contributions from diffusion and transport.

In biological systems diffusion prevails over active transport in supplying material over short distances. An estimation of the relative importance of diffusion and active transport at any given distance from a source can be obtained by examining the Péclet number, Pe. This dimensionless number is a ratio of the rate at which material is transported by an active process to the rate at which it is transported by diffusion. The Péclet number is given by VL/D, where V is transport velocity, L is the length under consideration, and D is the diffusion coefficient (26). It can range from 0 when there is diffusion but no active transport to ∞ when there is active transport but no diffusion. A Péclet number that is much less than 1 means greater importance for

diffusion and less for active transport, whereas a larger Péclet number implies a higher contribution from active transport to supplying material.

In our experiments tubulin has a Péclet number of 0.86 after 3 hr, during which it has traveled 281 μm, whereas neurofilament has traveled only 142 μm in the same time but, with its lower diffusion coefficient, has a Péclet number of 4.4. These numbers suggest that although there is a contribution from diffusion to our measurements in the squid axon, it is not nearly as dominant as in some of the previously reported photobleaching (12, 13, 41–43) and photoactivation (42, 44) experiments. In those experiments the short lengths of the detectable photobleached or photoactivation spots, and thus Péclet numbers, are several orders of magnitude less than those available in the squid axon. Therefore, unless the material of interest has a very low diffusion coefficient, observing movements over distances of only a few micrometers will make it extremely difficult to observe a measurable transport signal. Conversely, the much larger distances found in most radiolabeling experiments *in vivo*, typically greater than 10^4 μm, produce Péclet numbers that are larger than 40, making it easy to measure transport (4, 6). Although the contribution of diffusion is negligible in these longer axons used in experiments *in vivo*, making it easier to determine net transport rates, these systems do not lend themselves to pharmacological manipulations of the axons. Thus, the *in vivo* experiments are limited in their ability to answer questions regarding size, tracks, or motors.

The inverse relationship that diffusion and transport have with distance is an important reason that the squid giant axon provides a useful system for studying slow transport. Its length and large size allow direct injection of transport substrates, thereby providing information about their passive diffusion properties as well as their active transport behaviors. The squid model thus combines the best features of current *in vitro* and *in vivo* systems and should enable us to investigate the mechanisms for delivering essential axonal proteins.

We thank Jessica Ciralsky for her technical assistance along with Mark Terasaki, Bechara Kachar, Cathy Galbraith, and Sergey Popov for their helpful suggestions and comments.

1. Sabry, J., O'Connor, T. P. & Kirschner, M. W. (1995) *Neuron* **14,** 1247–1256.
2. Grafstein, B. & Forman, D. S. (1980) *Physiol. Rev.* **60,** 1167–1283.
3. Nixon, R. A. (1998) *Curr. Opin. Cell Biol.* **10,** 87–92.
4. Hoffman, P. N. & Lasek, R. J. (1975) *J. Cell Biol.* **66,** 351–366.
5. Lasek, R. J. (1986) *J. Cell Sci. Suppl.* **5,** 161–179.
6. Cancalon, P., Brady, S. T. & Lasek, R. J. (1988) *Brain Res.* **466,** 275–285.
7. Keith, C. H. (1987) *Science* **235,** 337–339.
8. Okabe, S. & Hirokawa, N. (1989) *Curr. Opin. Cell Biol.* **1,** 91–97.
9. Chang, S., Rodionov, V. I., Borisy, G. G. & Popov, S. V. (1998) *J. Neurosci.* **18,** 821–829.
10. Yoon, M., Moir, R. D., Prahlad, V. & Goldman, R. D. (1998) *J. Cell Biol.* **143,** 147–157.
11. Koehnle, T. J. & Brown, A. (1999) *J. Cell Biol.* **144,** 447–458.
12. Okabe, S. & Hirokawa, N. (1990) *Nature (London)* **343,** 479–482.
13. Okabe, S., Miyasaka, H. & Hirokawa, N. (1993) *J. Cell Biol.* **121,** 375–386.
14. Terasaki, M., Schmidek, A., Galbraith, J. A., Gallant, P. E. & Reese, T. S. (1995) *Proc Natl. Acad. Sci. USA* **92,** 11500–11503.
15. Gallant, P. E. (1988) *J. Neurosci.* **8,** 1479–1484.
16. Schnapp, B. J., Vale, R. D., Sheetz, M. P. & Reese, T. S. (1985) *Cell* **40,** 455–462.
17. Morris, R. L. & Hollenbeck, P. J. (1995) *J. Cell Biol.* **131,** 1315–1326.
18. Gallant, P. E. & Galbraith, J. A. (1997) *J. Neurotrauma* **14,** 811–822.
19. Crank, J. (1975) *The Mathematics of Diffusion* (Oxford Univ. Press, New York).
20. Seiler, M. & Weiss, D. G. (1987) *J. Pharmacol. Exp. Ther.* **242,** 277–283.
21. Brady, S. T., Tytell, M. & Lasek, R. J. (1984) *J. Cell Biol.* **99,** 1716–1724.
22. Baas, P. W. & Heidemann, S. R. (1986) *J. Cell Biol.* **103,** 917–927.
23. Luby-Phelps, K. (1994) *Curr. Opin. Cell Biol.* **6,** 3–9.
24. Berg, H. C. (1983) *Random Walks in Biology* (Princeton Univ. Press, Princeton, NJ).
25. Popov, S. & Poo, M. M. (1992) *J. Neurosci.* **12,** 77–85.
26. Vogel, S. (1996) *Life in Moving Fluids* (Princeton Univ. Press, Princeton, NJ).
27. Haak, R. A., Kleinhans, F. W. & Ochs, S. (1976) *J. Physiol.* **263,** 115–137.
28. Black, M. M. & Lasek, R. J. (1980) *J. Cell Biol.* **86,** 616–623.
29. Terada, S., Nakata, T., Peterson, A. C. & Hirokawa, N. (1996) *Science* **273,** 784–788.
30. Baas, P. W. & Brown, A. (1997) *Trends Cell Biol.* **7,** 380–384.
31. Hirokawa, N., Terada, S., Funakoshi, T. & Takeda, S. (1997) *Trends Cell Biol.* **7,** 384–388.
32. Weiss, D. G., Langford, G. M., Seitz-Tutter, D. & Keller, F. (1988) *Cell Motil. Cytoskeleton* **10,** 285–295.
33. Samson, F., Donoso, J. A., Heller-Bettinger, I., Watson, D. & Himes, R. H. (1979) *J. Pharmacol. Exp. Ther.* **208,** 411–417.
34. Langford, G. M., Kuznetsov, S. A., Johnson, D., Cohen, D. L. & Weiss, D. G. (1994) *J. Cell Sci.* **107,** 2291–2298.
35. Bearer, E. L. & Reese, T. S. (1999) *J. Neurocytol.,* in press.
36. Kravit, N. G., Regula, C. S. & Berlin, R. D. (1984) *J. Cell Biol.* **99,** 188–198.
37. Morris, J. R. & Lasek, R. J. (1982) *J. Cell Biol.* **92,** 192–198.
38. Okabe, S. & Hirokawa, N. (1988) *J. Cell Biol.* **107,** 651–664.
39. Keith, C. H. & Farmer, M. A. (1993) *Cell Motil. Cytoskeleton* **25,** 345–357.
40. Lasek, R. J., Garner, J. A. & Brady, S. T. (1984) *J. Cell Biol.* **99,** 212s–221s.
41. Okabe, S. & Hirokawa, N. (1992) *J. Cell Biol.* **117,** 105–120.
42. Okabe, S. & Hirokawa, N. (1993) *J. Cell Biol.* **120,** 1177–1186.
43. Takeda, S., Okabe, S., Funakoshi, T. & Hirokawa, N. (1994) *J. Cell Biol.* **127,** 173–185.
44. Funakoshi, T., Takeda, S. & Hirokawa, N. (1996) *J. Cell Biol.* **133,** 1347–1353.